Electron-hole pair creation and conversion efficiency in radioisotope microbatteries

G. Lioliou* and A.M. Barnett

Space Research Group, School of Mathematical and Physical Sciences, University of Sussex, Falmer, Brighton, BN1 9QT, UK

ABSTRACT

The ultimate conversion efficiency of semiconductor radioisotope microbatteries is set by the average energy consumed in the creation of an electron-hole pair, ω. Although the Klein relationship between ω and semiconductor bandgap, E_g, is widely cited, not only for radioisotope microbatteries, but indeed for a multitude of fields requiring accurate values of ω, its validity has been recently questioned; new experimental measurements have resulted in the refined Bertuccio-Maiocchi-Barnett (BMB) relationship. Here, it is shown that the new relationship indicates the ultimately achievable conversion efficiencies of radioisotope microbatteries are much greater than had ever been expected. For example, it appears possible to produce planar ^{63}Ni-Diamond radioisotope microbatteries with output powers 130× greater than has currently been achieved. The ultimate limit for batteries employing pore channels rather than planar designs is likely to be even greater still. These new findings open the possibility of using radioisotope microbatteries in a far greater variety of applications than has been traditionally assumed. As well as being of direct applicability to radioisotope microbatteries, the results highlight the need to reconsider the use of the Klein relationship in all fields that currently employ it.

1. Introduction

The average energy consumed in the creation of an electron-hole pair, ω, sets the ultimate conversion efficiency of semiconductor radioisotope microbatteries [1,2]. The parameter also has important implications for X-ray excitonics [3,4], radiation detection [5-8], photovoltaics [9], and advanced future optoelectronic devices [10].

*Corresponding author. Tel.: +44 (0) 1273 872568. E-mail address: G.Lioliou@sussex.ac.uk

Radioisotope microbatteries convert radioactive emissions from an integrated radioisotope into electrical energy by means of photo-, alpha-, or beta- generated electron-hole pairs in a semiconductor junction [2,11-14]. Such batteries benefit from long life-times and high energy densities, governed by the emission characteristics of the radioisotope utilized. The theoretical maximum (ultimate) conversion efficiency for a radioisotope microbattery, defined as the upper limit of the semiconductor device efficiency in converting the radiation quanta to electrical energy, assuming an ideal semiconductor device,

$$\eta_{sU} = \frac{E_g}{\omega}, \tag{1}$$

where E_g is the bandgap energy of the semiconductor, is independent of the radioisotope source, and, dependent upon only the bandgap energy and the average energy consumed in the creation of an electron-hole pair in the semiconductor junction. Eq. (1) that the use of a wide bandgap semiconductor for the conversion device of a radioisotope microbattery is advantageous. The Klein relationship [15],

$$\omega = E_g + \frac{9}{5}E_g + r(\hbar\omega_R), \tag{2}$$

builds on work by Shockley [16] and McKay [17]. The second and third terms of Eq. (2) are said to represent the residual kinetic energy and the optical phonon losses (0.5 eV < r ($\hbar\omega_R$) < 1.0 eV, where r is "an adjustable parameter" [15]) respectively. The Klein relationship has been used widely to calculate ω, and thus to predict the maximum conversion efficiency of radioisotope microbatteries [13,18-20] as well as for other purposes in a multitude of fields.

In this work the shortcomings of the Klein relationship are first discussed, while a refined relationship between the bandgap and the electron-hole pair creation energy, the Bertuccio-Maiocchi-Barnett (BMB) relationship, which resulted from carefully conducted measurements on modern semiconductor materials, is introduced. The ultimate conversion efficiency of radioisotope

microbatteries as a function of bandgap energy of the conversion device and the conversion efficiency of radioisotope microbatteries employing two typical laboratory radioisotope sources, is then calculated using both the Klein and the BMB relationship; the results are compared. Finally, to explore the maximum potentially achievable performance of radioisotope microbatteries, the upper limit of the output power of an optimized ^{63}Ni-diamond battery is calculated. It should be noted here that the main focus of the current work is the semiconductor conversion efficiency and its relationship with the average electron-hole pair creation energy, whereas the two other efficiencies relevant to radioisotope microbatteries, namely the radioisotope source efficiency and the coupling efficiency, are excluded from the following discussion.

2. Shortcomings of the Klein relationship

The Klein relationship was derived from a collection of measurements on early semiconductors collated from the literature as it stood prior to October 1967. With scant data available, no considerations were made for initiating radiation type or energy, nor of temperature or quality of semiconductor material. It was recognised at the time that this may affect the validity of the apparent relationship [15], although the work of Shockley [16] stated explicitly that ω "was independent of the nature of the particle" and dependent "only on its energy" citing the work of Grainger et al. [21] and McKay and McAfee [22]. It is accepted now that as well as varying with E_g, ω also depends on material temperature [23-28] and initiating photon energy, E, at soft X-ray energies ($E < 0.5$ keV in Si [29]) and when E is close to the energies of the absorption edges of the material [29]; variation of ω at hard X-ray energies appears to be small [29]. Incomplete charge collection in semiconductor materials of poor quality (common in the 1960s) is also known to produce anomalously high apparent values of ω [25]. A dependence of ω upon initiating quantum type is still discussed; apparent variations may be due to charge collection efficiencies < 1 in the semiconductor structures used to measure the parameter [25] as well as backscatter effects [15]. However, even excluding those phenomena, it is reasonable to assume that a slightly different apparent ω value may result in some cases. An X-ray or γ-ray photon deposits its energy in a single instance when Compton scatting and pair production are negligible, whereas beta- and alpha- particles deposit their energy along the length

of their absorption tracks in a series of energy loss events. As such, it is reasonable to assume that a slightly larger apparent ω value may result if it is computed on the basis of the initial energy of the beta- or alpha- particle being divided by the total number of electron-hole pairs produced over the entire track, rather than by consideration of each loss event separately. Whilst the former may be expedient for some applications – and easier to measure experimentally – the larger apparent ω computed in this way would be incorrect since the multiple energy loss events along the track give rise to multiple (per initial quantum) partitionings of deposited energy between electron-hole pairs and other processes (e.g. phonon loses), even if the events themselves (as well as the electron-hole pairs created in each event) are not strictly independent of each other [7].

The validity of the Klein relationship was first questioned when more materials were added to the Klein plot. Owens and Peacock [30] included ω values (without uncertainties) for 22 materials obtained from the literature. As per the original Klein plot, no control was made of quantum energy or type or material quality or temperature. However, at least some of the data points included were reliable (notably those for Ge and Si [24] and GaAs [25]). Based on the distribution of the data, Owens and Peacock suggested the presence of two Klein branches each forced to have a gradient identical to that suggested by Klein [15] but with different intercepts, one of which was unphysical in the Shockley-Klein model [15,16] since it indicated a negative energy loss to optical phonons.

The first material to match neither Klein branch was $Al_{0.8}Ga_{0.2}As$; using high quality material and X-rays, ω was measured in $Al_{0.8}Ga_{0.2}As$ at a controlled temperature of 294 K [31], and then as a function of temperature [23]. The values of $\omega(E_g)$ at 300 K for Si, Ge, GaAs, and $Al_{0.8}Ga_{0.2}As$ formed a straight line with a gradient and intercept [23] different to those predicted by Klein [15]. $\omega(T)$ was measured subsequently in $Al_{0.2}Ga_{0.8}As$ [26], $Al_{0.6}Ga_{0.4}As$ [32], $Al_{0.52}In_{0.48}P$ [27], and $In_{0.5}Ga_{0.5}P$ [28] these values at 300 K were used along with those of Ge and Si [24] and GaAs [25] to refine the relationship between ω and E_g suggested from the $Al_{0.8}Ga_{0.2}As$ measurements. The most recently refined Bertuccio-Maiocchi-Barnett (BMB) relationship [32],

$$\omega = (1.54 \pm 0.07)\, E_g + (1.89 \pm 0.12)\,, \tag{3}$$

is quantitatively different from the Klein relationship (**Eq. 2**) and suggests that the mechanisms proposed by Shockley [16] and Klein [15] may be incorrect or at least incorrectly apportioned in their contributions. In contrast to the Klein relationship, the BMB relationship (**Eq. 3**) resulted from measurements at a controlled temperature (300 K) using only high-quality materials (with negligible incomplete charge collection) and only X-ray and γ-ray photons (with energies low enough that Compton scatting and pair production processes were negligible). It should be noted that the BMB relationship shows the dependence of ω upon E_g, where ω is average energy consumed in the creation of an electron-hole pair, ω, on a per interaction basis. Whilst alpha and beta particles may undergo multiple interactions, thus leading to a slightly higher apparent average electron-hole pair creation energy on a per particle (cf. per interaction) basis, the limit for their charge creation (and hence theoretical maximum (ultimate) conversion efficiency is still set by ω). However, it is anticipated that Monte Carlo computer simulations and experimental results may be reported in future which quantify the difference between ω and the average electron-hole pair creation energy on a per particle basis for particles which do not lose all of their energy in a single interaction event, such as alpha and beta particles. The latter (the average electron-hole pair creation energy on a per particle basis) is anticipated to be a function of particle energy as well as dependent on the elemental composition and crystalline structure of the material with which it is interacting. Once such values are available, it will be informative to compare the conversion efficiencies they predict with those predicted using ω. The form of **Eq. 3**, which still follows that long-known for gas-ionisation chambers [33], does not necessarily require a fundamental reconceptualization of the notion that the energy of the quanta are divided between electron-hole pairs and losses to the lattice [16,29,34,35]. However, it does highlight that the specifics of the apportionment warrant further exploration.

3. Results and discussion

3.1. Ultimate conversion efficiency

Whilst the mechanics of electron-hole pair creation are of fundamental importance, they are also of practical concern, as shown for radioisotope microbatteries in **Eq. 1**. Given **Eq. 3**, a significant revision to the ultimate conversion efficiencies expected of radioisotope microbatteries as a function

of the semiconductor bandgap is required. **Fig. 1** uses **Eq. 1** to show the ultimate conversion efficiency implied by the BMB relationship (**Eq. 3**) and compares it to that computed using the Klein relationship (**Eq. 2**) with $r(\hbar\omega_R) = 0.606$ [30].

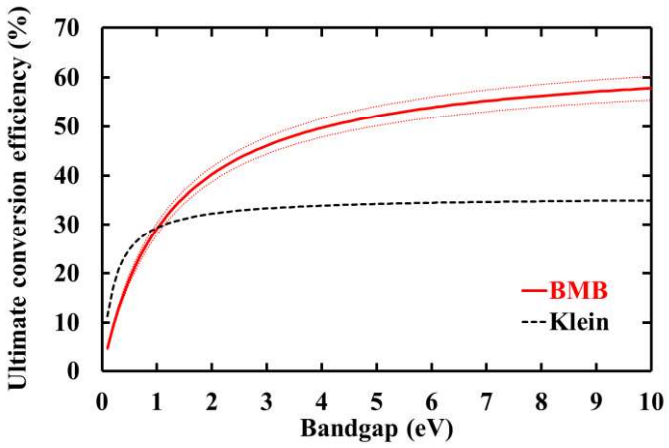

FIG. 1. Comparison between the ultimate conversion efficiencies predicted by the Klein [15] (---) and BMB [32] (—, with error bars) relationships for radioisotope microbatteries as a function of bandgap.

As shown in **Fig. 1**, the Klein relationship suggests that the ultimate conversion efficiency for radioisotope microbatteries saturates at 35 % when $E_g \geq 6.2$ eV. In contrast, the BMB relationship suggests greater conversion efficiencies than Klein when $E_g > 1.0$ eV, and that saturation does not occur within the range of conventional bandgap energies.

For diamond, $E_g = 5.5$ eV, Klein predicts a 34 % ultimate efficiency, whereas the BMB relationship predicts 53 % ± 2 %. Thus, it appears that the ultimate efficiency of diamond batteries is a factor of 1.5 greater than previously thought.

3.2. Conversion efficiency and upper limit of power output

It is informative to compute the semiconductor conversion efficiencies potentially achievable with two typical laboratory radioisotope sources used for characterization (one beta emitter, ^{63}Ni; one X-ray emitter, ^{55}Fe) and ten common semiconductor materials, since it is this value which radioisotope microbattery engineers strive to attain.

Radioisotope microbatteries with planar geometries and single side illumination were considered; each radioisotope source was assumed to be in direct contact with the top face of the semiconductor conversion device. Two typical laboratory radioisotope sources were considered, ^{63}Ni (a beta-particle emitter, endpoint energy = 66.9 keV [36]) and ^{55}Fe (an X-ray emitter, giving Mn Kα = 5.9 keV and Mn Kβ = 6.49 keV photons [37]). Ten common semiconductor materials were chosen for consideration: Si; GaAs; $Al_{0.2}Ga_{0.8}As$; $In_{0.5}Ga_{0.5}P$; $Al_{0.8}Ga_{0.4}As$; $Al_{0.52}In_{0.48}P$; 4H-SiC; $Al_{0.5}Ga_{0.5}N$; diamond; and c-BN. The structure of the conversion device was assumed to have a thickness large enough to ensure full absorption of the beta-particle or X-ray power incident upon the conversion device. The required conversion device thickness for efficient beta particle absorption depends on the energies of the beta particles in question as well as the specific semiconductor material used as the converter; for a ^{63}Ni radioisotope beta particle source (end point energy = 66 keV), the depth at which 87 % of all beta particle energy is fully absorbed, has been calculated previously to be 5 μm for GaAs and 9.5 μm for diamond, for example [18]. The required conversion device thickness for efficient X-ray photon absorption depends on the energy of the X-rays, the semiconductor density, and the mass absorption coefficient of the semiconductor material at that X-ray energy [38]; for an ^{55}Fe radioisotope X-ray source (primary X-ray emission Mn Kα = 5.9 keV), the depth at which 1/e of the X-rays is absorbed was calculated to be 12 μm for GaAs and 256 μm for diamond, for example. It should be noted here that thick conversion devices may suffer from poor quality materials resulting in reduced charge collection efficiencies. In addition, a backscatter coefficient = 0 was considered, thus enabling direct comparisons of different semiconductor materials. Partial absorption of the incident power and energy losses due to backscattering would reduce the coupling efficiency between the radioisotope source and the conversion device (≤ 1); however, real-world coupling efficiencies as high as 0.91 have been calculated for ^{63}Ni-diamond microbatteries [18]. Each conversion device was assumed to cover an area large enough that edge effects were negligible.

The ^{63}Ni radioisotope beta particle source was assumed to be 5 μm thick (with an area of 6.92 mm × 6.92 mm based on the details given [18], although the geometric area of the source is inconsequential for the analysis which follows here); this was found to be the optimal thickness to deliver maximum power, based on the radioisotope's energy spectrum and material density [18].

Although highly pure ^{63}Ni radioactive material may have a specific activity of up to 56.8 Ci/g, typical commercially available laboratory ^{63}Ni radioactive material are less pure; a purity of 50 % was assumed for the calculations, thus giving a specific activity of 28.4 Ci/g i.e. an activity of 126 mCi [18]. The beta particle power incident to the conversion device has been previously calculated using Monte Carlo simulations [18] and was found to be 2.68 μW cm^{-2}. The ^{55}Fe radioisotope X-ray source was assumed to be a circular disk of 7.92 mm diameter; similarly to the ^{63}Ni radioisotope beta particle source, the geometric area of the ^{55}Fe radioisotope X-ray source is inconsequential for the analysis which follows here. It had an activity at its surface of 100 mCi, employing a 250 μm thick Be window to absorb the emitted Auger electrons as this is a common arrangement for laboratory sealed sources. The X-ray power incident to the conversion device was calculated taking into account the activity and the area of the source, the X-ray attenuation through the Be window, as well as the energies of the emitted X-ray photons and their emission probabilities [37]; it was found to be 0.89 μW cm^{-2}. The schematic diagram of the two types of the radioisotope microbatteries considered can be seen in **Fig. 2**.

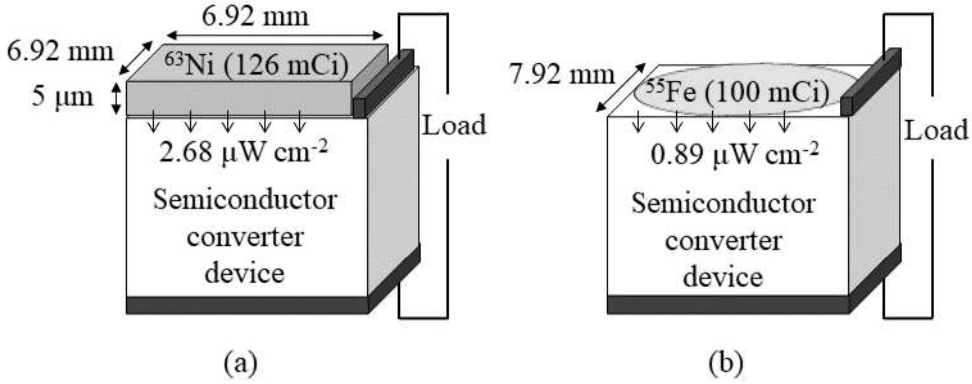

FIG. 2. Schematic diagram of the (a) ^{63}Ni radioisotope beta particle source and (b) ^{55}Fe radioisotope X-ray source based microbatteries considered for the calculations. The geometry of the source in each case is inconsequential for the analysis presented here; the same power incident on the conversion device may be realised via the use of radiation sources of different geometries. The schematics are given to aid the reader's conceptualisation rather than to reflect specific real world microbattery designs.

To enable comparison, ω was calculated using both the Klein (**Eq. 2**) and BMB (**Eq. 3**) relationships. The saturation current density was calculated using a simplified empirical relationship between the saturation current and $E_g(T)$ [39]. The short circuit current density, the open circuit voltage, V_{OC}, and the fill factor, F_F, (each of which is dependent upon ω) were calculated given the illumination characteristics of the two sources. Finally, the upper limit of the semiconductor conversion efficiency,

$$\eta_S = \frac{V_{OC}F_F}{\omega}, \tag{4}$$

was computed by applying the detailed balance limit derived by Shockley and Queisser [40], and excluding Auger recombination, band tail recombination, recombination in the bulk, at interfaces, and at surface defects, and contact losses [9]; the results are shown in **Fig. 3**.

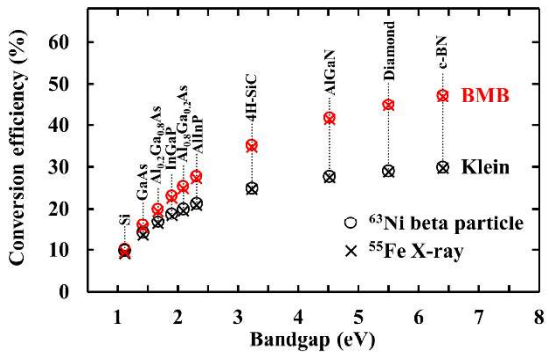

FIG. 3. Comparison between the semiconductor conversion efficiencies predicted by the Klein [15] (○ and ×) and BMB [32] (○ and ×) relationships for ^{63}Ni beta particle (○ and ○) and ^{55}Fe X-ray (× and ×) radioisotope microbatteries based on Si; GaAs; $Al_{0.2}Ga_{0.8}As$; $In_{0.5}Ga_{0.5}P$; $Al_{0.8}Ga_{0.4}As$; $Al_{0.52}In_{0.48}P$; 4H-SiC; $Al_{0.5}Ga_{0.5}N$; diamond; c-BN.

The upper limit of the semiconductor conversion efficiencies shown in **Fig. 2** for the X-ray-voltaic batteries was slightly lower than those for the beta-voltaic batteries, this was due to the lower illumination power of the typical ^{55}Fe radioisotope X-ray source (0.89 μW cm^{-2}) cf. that of the typical ^{63}Ni radioisotope beta particle source (2.68 μW cm^{-2}). Whilst the semiconductor conversion efficiency computed for radioisotope microbatteries employing Si converter devices did not differ between the BMB (= 10.2 % ± 0.4 % with ^{63}Ni) and Klein (= 9.8 % with ^{63}Ni) relationships, most radioisotope microbattery designs employ wide bandgap semiconductor converters. The difference was substantial as E_g increased: e.g. for ^{63}Ni-GaAs (E_g = 1.42 eV) 14.2 % (Klein) and 16.0 % ± 0.6 % (BMB); for ^{63}Ni-diamond (E_g = 5.5 eV) 29 % (Klein) and 45 % ± 2 % (BMB). Thus, the upper limit of the semiconductor conversion efficiency for a ^{63}Ni-diamond microbattery of the structure described here is expected to be 55 % greater than was previously thought.

Given these calculations it is possible to compute the upper limit of the power output per unit area of illumination, P_{max}, for the planar microbattery structure considered here. The maximum power output per unit area of illumination was 0.43 μW cm^{-2} ± 0.02 μW cm^{-2} for ^{63}Ni-GaAs and 1.21 μW cm^{-2} ± 0.05 μW cm^{-2} for ^{63}Ni-diamond, when the BMB relationship was used, in contrast to 0.38 μW cm^{-2} and 0.78 μW cm^{-2} using the Klein relationship. The availability of highly enriched ^{63}Ni would enable even greater power outputs: at 100 % enrichment (5.36 μW cm^{-2} incident on the converter), the battery would output 2.42 μW cm^{-2}. Although production of isotopically-pure 100 % enriched ^{63}Ni is still considered an expensive and challenging task, a scheme was proposed recently to enrich ^{63}Ni content to 80-90 % [41].

A prototype multi-layer ^{63}Ni-diamond microbattery has been reported previously that achieves ~0.0186 μW cm^{-2} from an irradiance of 0.5 μW cm^{-2}, giving 10 μW cm^{-3}, enough to power a cardiac pacemaker [42]. The semiconductor conversion efficiency ranged between 4.5 % and 6 % [42] (cf. the 45 % ± 2 % ultimate limit predicted by the BMB relationship). Given the BMB relationship and highly enriched ^{63}Ni (100 %), the ultimate limit (power output per unit area illuminated) for multi-layer ^{63}Ni-diamond batteries appears to be 130 times greater (i.e. 2.42 μW cm^{-2}) than has so far been achieved; this translates to a power density of 1300 μW cm^{-3} (= 1.3 W l^{-1}) which is an astounding figure and far greater than was ever previously considered achievable with such

devices, thus the range of potential applications for radioisotope microbatteries is broader than was expected. It should be noted here that this calculated ultimate limit of conversion efficiency for ^{63}Ni-diamond batteries is unlikely to be realised in practice since it excludes non-ideal behaviour of real microbatteries (e.g. recombination, scattering, series and shunt resistances). Nevertheless, it is important for device physicists and engineers to compare the efficiencies achieved with their real-world batteries to this ultimate efficiency value since through doing so, it is possible to quantify the negative contributions made by the various lossy processes and, as such, work to reduce their impacts on real-world battery designs.

Utilizing 3D structures (e.g. pore channels within the conversion device) to increase the effective surface area of illumination [43] [44] has been shown to increase battery conversion efficiencies by a factor of ten compared to those of planar structure [12], and thus may provide a route to increasing this power density even further.

4. Conclusions

The ultimate conversion efficiency, power output, and power density of radioisotope microbatteries is shown to be far greater than had previously been supposed. In principle, a ^{63}Ni-diamond microbattery could have a semiconductor conversion efficiency of up to 45 % ± 2 %, and a power output density as high as 1300 μW cm^{-3} (= 1.3 W l^{-1}) when employing highly enriched ^{63}Ni and a multi-planar configuration (i.e. utilizing beta-particles emitted from both sides of the radioisotope foil). Furthermore, it is apparent that the detailed physics of electron-hole pair creation in semiconductor materials in response to X-ray photons and other radiation quanta with similar energies still needs further exploration. This is important not just for radioisotope microbatteries but indeed all applications which require accurate values of ω. Recently reported data obtained with modern semiconductor materials and experiments carefully controlled for parameters such as temperature and quanta type have shown that the previously widely-used Klein relationship [15] is incorrect; the relationship between electron-hole pair creation energy and bandgap energy is better described by the Bertuccio-Maiocchi-Barnett (BMB) relationship [32]. However, like the Klein relationship, the BMB relationship is semi-empirical; work is still required to understand the specific mechanisms of

apportionment of photon energy between electron-hole pairs and the various loss mechanisms, particularly as a function of bandgap and temperature.

Acknowledgements

This work was supported in part by Science and Technology Facilities Council, UK, Grants ST/P001815/1 and ST/T000910/1 (PI A.M.B.). A.M.B also acknowledges funding received from The Leverhulme Trust, UK, in the form of a 2016 Philip Leverhulme Prize.

Data availability

Whilst all data from the study and the findings are contained within the paper, further reasonable requests for information may be addressed to the authors.

CRediT Author Statement

G. Lioliou: Validation, Formal analysis, Data Curation, Writing – Original Draft, Writing – Review and Editing, Visualization; **A.M. Barnett:** Conceptualization, Methodology, Validation, Formal analysis, Investigation, Resources, Data Curation, Writing – Original Draft, Writing – Review and Editing, Visualization, Supervision, Project administration, Funding Acquisition.

REFERENCES

[1] J. Dixon, A. Rajan, S. Bohlemann, D. Coso, A.D. Upadhyaya, A. Rohatgi, S. Chu, A. Majumdar, and S. Yee, Evaluation of a Silicon ^{90}Sr Betavoltaic Power Source, Sci. Rep. 6 (2016) 38182.

[2] L.C. Olsen, P. Cabauy, and B.J. Elkind, Betavoltaic power sources, Phys. Today 65 (2012) 35.

[3] S.W. Koch, M. Kira, G. Khitrova, and H.M. Gibbs, Semiconductor excitons in new light, Nat. Mater. 5 (2006) 523–531.

[4] A. Moulet, J.B. Bertrand, T. Klostermann, A. Guggenmos, N. Karpowicz, and E. Goulielmakis, Soft x-ray excitonics, Science 357 (2017) 1134–1138.

[5] S. Shrestha, R. Fischer, G.J. Matt, P. Feldner, T. Michel, A. Osvet, I. Levchuk, B. Merle, S. Golkar, H. Chen, S.F. Tedde, O. Schmidt, R. Hock, M. Rührig, M. Göken, W. Heiss, G. Anton, and

C.J. Brabec, High-performance direct conversion X-ray detectors based on sintered hybrid lead triiodide perovskite wafers, Nat. Photon. 11 (2017) 436–440.

[6] J. Liu, F. Xia, D. Xiao, F.J. García de Abajo, and D. Sun, Semimetals for high-performance photodetection, Nat. Mater. 19 (2020) 830–837.

[7] U. Fano, Ionization Yield of Radiations. II. The Fluctuations of the Number of Ions, Phys. Rev. 72 (1947) 26–29.

[8]. J. David, The staircase photodiode, Nat. Photon. 10 (2016) 364–366.

[9] A. Polman, M. Knight, E.C. Garnett, B. Ehrler, and W.C. Sinke, Photovoltaic materials: Present efficiencies and future challenges, Science 352 (2016) aad4424-1–aad4424-10.

[10] T.B. Arp, D. Pleskot, V. Aji, and N.M. Gabor, Electron–hole liquid in a van der Waals heterostructure photocell at room temperature, Nat. Photon. 13 (2019) 245.

[11] P. Rappaport, The Electron-Voltaic Effect in p–n Junctions Induced by Beta-Particle Bombardment, Phys. Rev. 93 (1954) 246–247.

[12] W. Sun, N.P. Kherani, K.D. Hirschman, L.L. Gadeken, P.M. Fauchet, A Three-Dimensional Porous Silicon p-n Diode for Betavoltaics and Photovoltaics, Adv. Mater. 17 (2005) 1230–1233.

[13] M.V.S. Chandrashekhar, C.I. Thomas, H. Li, M.G. Spencer, and A. Lal, Demonstration of a 4H-SiC betavoltaic cell, Appl. Phys. Lett. 88 (2006) 033506.

[14] S. Butera, G. Lioliou, A.B. Krysa, and A.M. Barnett, $Al_{0.52}In_{0.48}P$ ^{55}Fe x-ray-photovoltaic battery, J. Phys. D: Appl. Phys. 49 (2016) 355601.

[15] C.A. Klein, Bandgap Dependence and Related Features of Radiation Ionization Energies in Semiconductors, J. Appl. Phys. 39 (1968) 2029–2038.

[16] W. Shockley, Problems related to p-n junctions in silicon, Solid State Electron. 2 (1961) 35–60.

[17] K.G. McKay, Electron-Hole Production in Germanium by Alpha-Particles, Phys. Rev. 84 (1951) 829–832.

[18] S.I. Maximenko, J.E. Moore, C.A. Affouda, and P.P. Jenkins, Optimal Semiconductors for ^{3}H and ^{63}Ni Betavoltaics, Sci. Rep. 9 (2019) 10892.

[19] C.J. Eiting, V. Krishnamoorthy, S. Rodgers, and T. George, Demonstration of a radiation resistant, high efficiency SiC betavoltaic, Appl. Phys. Lett. 88 (2006) 064101.

[20] L.C. Olsen, Review of betavoltaic energy conversion, Proc. SPRAT 12 (1993) 256–267.

[21] R.J. Grainger, J.W. Mayer, J.S. Wiggins, and S.S. Friedland, Further Characteristics of the Solid-State Ionization Chamber, Bull. Amer. Phys. Soc. 5 (1960) 265.

[22] K.G. McKay, and K.B. McAfee, Electron Multiplication in Silicon and Germanium, Phys. Rev. 91 (1953) 1079–1084.

[23] A.M. Barnett, J.E. Lees, and D.J. Bassford, Temperature dependence of the average electron-hole pair creation energy in $Al_{0.8}Ga_{0.2}As$, Appl. Phys. Lett. 102 (2013) 181119.

[24] R.H. Pehl, F.S. Goulding, D.A. Landis, and M. Lenzlinger, Accurate determination of the ionization energy in semiconductor detectors, Nucl. Instrum. Methods 59 (1968) 45–55.

[25] G. Bertuccio, and D. Maiocchi, Electron-hole pair generation energy in gallium arsenide by x and γ photons, J. Appl. Phys. 92 (2002) 1248–1255.

[26] M.D.C. Whitaker, S. Butera, G. Lioliou, and A.M. Barnett, Temperature dependence of $Al_{0.2}Ga_{0.8}As$ X-ray photodiodes for X-ray spectroscopy, J. Appl. Phys. 122 (2017) 034501.

[27] S. Butera, G. Lioliou, A.B. Krysa, and A.M. Barnett, Measurement of the electron–hole pair creation energy in $Al_{0.52}In_{0.48}P$ using X-ray radiation, Nucl. Instrum. Methods Phys. Res. A 879 (2018) 64–68.

[28] S. Butera, G. Lioliou, A.B. Krysa, and A.M. Barnett, Temperature characterisation of spectroscopic InGaP X-ray photodiodes, Nucl. Instrum. Methods Phys. Res. A 908 (2018) 277–288.

[29] G.W. Fraser, A.F. Abbey, A. Holland, K. McCarthy, A. Owens, and A. Wells, The X-ray energy response of silicon Part A. Theory, Nucl. Instrum. Methods Phys. Res. A 350 (1994) 368–378.

[30] A. Owens, and A. Peacock, Compound semiconductor radiation detectors, Nucl. Instrum. Methods Phys. Res. A 531 (2004) 18–37.

[31] A.M. Barnett, J.E. Lees, D.J. Bassford, and J.S. Ng, Determination of the electron-hole pair creation energy in $Al_{0.8}Ga_{0.2}As$, J. Instrum. 7 (2012) P06016.

[32] M.D.C. Whitaker, G. Lioliou, A.B. Krysa, and A.M. Barnett, $Al_{0.6}Ga_{0.4}As$ X-ray avalanche photodiodes for spectroscopy, Semicond. Sci. Technol. 35 (2020) 095026.

[33] E. Baldinger, and W. Czaja, On the energy expended per electron-hole-pair produced in p-n-junction-detectors, Nucl. Instrum. Methods 10 (1961) 237–239.

[34] F. Gao, L.W. Campbell, R. Devanathan, Y. Xie, L.R. Corrales, A.J. Peurrung, and W.J. Weber, Monte Carlo method for simulating γ-ray interaction with materials: A case study on Si, Nucl. Instrum. Methods Phys. Res. A 579 (2007) 292–296.

[35] F. Gao, L.W. Campbell, R. Devanathan, Y.L. Xie, Y. Zhang, A.J. Peurrung, and W.J. Weber, Gamma-ray interaction in Ge: A Monte Carlo simulation, Nucl. Instrum. Methods Phys. Res. B 255 (2007) 286–290.

[36] B. E. Zimmerman, and R. Collé, Standardization of ^{63}Ni by 4πβ Liquid Scintillation Spectrometry With ^{3}H-Standard Efficiency Tracing, J. Res. Natl. Inst. Stand. Technol. 102 (1997) 455–477.

[37] U. Schötzig, Half-Life and X-ray Emission Probabilities of ^{55}Fe, Appl. Radiat. Isot. 53 (2000) 469–472.

[38] J.H. Hubbell, Photon Mass Attenuation and Energy Absorption Coefficients from 1 keV to 20 MeV, Int. J. Appl. Radiat. Isotopes 33 (1982) 1269–1290.

[39] M.A. Green, Solar Cells: Operating Principles, Technology, and System Applications, Prentice-Hall, New Jersey, 1982.

[40] W. Shockley, and H.J. Queisser, Detailed Balance Limit of Efficiency of p- n Junction Solar Cells, J. Appl. Phys. 32 (1961) 510–519.

[41] B. Bryskin, A. Pustovalov, L. Tsvetkov, V. Fedorov, and A. Kostylev, Highly Enriched Nickel-63 Radionuclide for β-Voltaic Nuclear Batteries, Energy Technol. 2 (2014) 210–214.

[42] V.S. Bormashov, S.Yu. Troschiev, S.A. Tarelkin, A.P. Volkov, D.V. Teteruk, A.V. Golovanov, M.S. Kuznetsov, N.V. Kornilov, S.A. Terentiev, and V.D. Blank, High power density nuclear battery prototype based on diamond Schottky diodes, Diam. Relat. Mater. 84 (2018) 41–47.

[43] K. Hogan, M. Litz, and F. Shahedipour-Sandvik, 3D GaN-based betavoltaic device design with high energy transfer efficiency, Appl. Radiat. Isot. 145 (2019) 154–160.

[44] C. Yue, J. Li, and L. Lin, Fabrication of Si-based three-dimensional microbatteries: A review, Front. Mech. Eng. 12 (2017) 459–476.